Original article

Interannual Variability of Thermal Characteristics of the Upper 1000-meter Layer in the Extratropical Zone of the Northwestern Part of the Pacific Ocean at the Turn of the XX–XXI Centuries

I. D. Rostov ✉, E. V. Dmitrieva, N. I. Rudykh

V. I. Il'ichev Pacific Oceanological Institute, Far Eastern Branch of Russian Academy of Sciences, Vladivostok, Russian Federation
✉ *rostov@poi.dvo.ru*

Purpose. The purpose of the study is to determine the trends and the spatio-temporal features of interannual changes in the sea surface temperature (SST) and in the upper 1000-meter layer in the extratropical zone of the northwestern Pacific Ocean, and to analyze their possible causal relationships with the large-scale and regional processes in the ocean and atmosphere over the certain phases of the modern period of global warming.
Methods and Results. To analyze the NOAA climatic data sets, the methods of cluster, correlation and regression analysis, and also the apparatus of empirical orthogonal functions were used. The results obtained made it possible to characterize the trends in interannual dynamics of thermal characteristics of the upper, intermediate and deep layers in certain areas under various conditions of the 20-year phases of the 40-year period of modern climate changes, and to quantify their features and statistical significance.
Conclusions. In general, in the above region during both phases of the modern period of climate changes, positive statistically significant trends were observed in the annual average SST, the values of which in 1982–2000 were 1.3–1.5 times higher than those in 2000–2021. During the second period, the area of positive SST trends decreased significantly and was localized in the northwestern part of the area under study. In contrast to the SST, at the same period, positive trends of the water column temperature in the upper 1000-m layer were traced over most of the area under study. The correlations between the variations in the ocean upper layer heat content and the processes in the ocean and atmosphere are most extensively manifested through the climatic indices NPGO, PDO, WP, PTW, and the anomalies in the geopotential field ΔH_{500}.

Keywords: northwestern part of the Pacific Ocean, extratropical zone, modern climate changes, regional features, water temperature, warming trends, climate indices, correlations

Acknowledgments: The study was carried out within the framework of the Comprehensive Interdepartmental Program "Ecological Safety of Kamchatka: Study and Monitoring of Hazardous Natural Phenomena and Human Impacts" (NIOKTR 122012700198-9).

For citation: Rostov, I.D., Dmitrieva, E.V. and Rudykh, N.I., 2023. Interannual Variability of Thermal Characteristics of the Upper 1000-meter Layer in the Extratropical Zone of the Northwestern Part of the Pacific Ocean at the Turn of the XX–XXI Centuries. *Physical Oceanography*, 30(2), pp. 141-159. doi:10.29039/1573-160X-2023-2-141-159

DOI: 10.29039/1573-160X-2023-2-141-159

Introduction

In the conditions of modern global warming, the main trends in the interannual and interdecadal variability of the thermal characteristics of ocean waters are both a reflection of the natural cyclicity and internal dynamics of the *ocean* –

atmosphere – continent climate system and a consequence of its energy imbalance as a result of increasing anthropogenic impact on these geospheres, leading to the excess heat accumulation [1, 2]. One can observe separate phases with different warming rates, formed during changes in climatic regimes, characteristics of large-scale atmospheric and oceanic circulation, remote impact and under the influence of local physical and geographical conditions [3, 4].

Some decades, called accelerated warming phases, are characterized by a rapid increase in the global mean surface air temperature (T_a) and sea surface temperature (SST), others are characterized by a weakening of warming trends, or phases of a break in this process [5]. Thus, at the turn of the 20th –21st centuries there were shifts in climate regime of the planet towards accelerated warming in the late 1970s [3]. It was followed by a pause (hiatus), which started in the late 1990s and global warming during the first decade of the 21st century slowed down or even stopped [3, 5, 6]. At the same time, this pause is the result of the heat redistribution within and between the oceans, and not an indicator of changes in the warming rate of the entire Earth [7], the trends of which keep dominating [1]. Approximately from 2012, global surface temperatures have started to rise above climate norms [1] again. The area under consideration covers the waters of the western Bering Sea in the north, the cells of the western subarctic cyclonic gyre in the center, the Kuroshio-Oyashio energetically active zone (EAZO) in the southwest, and the areas of the transitional interstructural zone and the Kuroshio Extension in the south. It contains zones of subarctic and subtropical water structures and their modifications, separated by a subarctic front and a mixing zone, the characteristics of which, as well as the scheme of the main currents of the area, are well-studied [8–11]. Long range, atmosphere and ocean circulation features are the causes of significant differences in weather and climate conditions in this area. Here they mainly depend on the interaction of three main baric formations that are seasonal atmospheric action centers (AAC): the Aleutian minimum (Aleutian depression), the North Pacific (Hawaiian) maximum and the Siberian winter anticyclone, which determine the characteristics of the wind field and the state of the upper layer of the ocean. An important role in the formation of large-scale anomalies in the thermal characteristics of the atmosphere and ocean and in the thermal regime of the study area belongs to the Kuroshio-Oyashio EAZO. It is associated with an increase in heat and moisture fluxes from the ocean surface as a result of heat advection from the tropics to temperate and high latitudes and its redistribution between different regions. EAZO has the most important influence on the processes taking place not only in the adjacent areas of the ocean, but also in the Earth's climate system [4, 12].

In the interannual variability of SST anomalies (SSTA), the heat content of the upper layers of the ocean and atmospheric pressure, the influence of several main dominant modes, large-scale modes of oscillations in the ocean-atmosphere system,

[1] Pörtner, H.-O., Roberts, D.C., Masson-Delmotte, V., Zhai, P., Tignor, M., Poloczanska, E., Mintenbeck, K., Alegria, A., Nicolai, M. [et al.], eds., 2019. *IPCC Special Report on the Ocean and Cryosphere in a Changing Climate.* 755 p. In press. Available at: https://www.ipcc.ch/report/srocc [Accessed: 9 June 2022].

caused by both its internal variability and remote influence, is traced [2, 4]. They are parameterized by the corresponding climate indices (CI): AMO, IPO, NP, NPGO, PDO, SOI and WP [13, 14]. The Kuroshio Extension flow fluctuations and the position of the frontal zones make a significant contribution to the water temperature (T_w) variations at the surface and in the underlying layers [2, 15, 16]. The internal variability of these modes, as well as individual CI, is a combination of various processes [2] and is determined by the AAC position and severity in different seasons, while the remote impact is determined by planetary-scale processes [14].

The area under consideration is a specific indicator and a key to understanding current ecosystem trends observed in the Pacific Ocean, where climate signals can be detected earlier than subsequent changes in the climate regime [11, 17]. In the past four decades, the highest rate of T_a and SST increase within the entire Pacific Ocean basin was noted in its water area, and the trend contribution to the total dispersion of the average annual SST reached 30–40% [4, 18]. The greatest trends in these parameters were observed in the western Bering Sea and near the eastern coast of Kamchatka. At the same time, in a number of regions of the northwestern Pacific Ocean, there were trends of the T_w increase at different horizons [17] and in the heat content of the upper 700-m layer [2].

Recent years have become the warmest in the history of observations, which could not but affect the state of the region ecosystems. In the autumn of 2020, an ecological disaster occurred in the Avacha Bay waters and in other areas of the southeastern coast of Kamchatka, accompanied by a change in color and the appearance of foam on the water surface and led to the mass death of marine hydrobionts (up to 95% of benthos)[2] [19]. Similar phenomena, caused by an outbreak of mass blossom of harmful algae and called "red tides", were observed in the Kamchatka bays in some years and earlier; in 2021 they repeated again in the area of the Southern Kuril Islands and near the east coast of Hokkaido Island. In the era of modern climate change, the frequency and scale of "red tides" have significantly increased, and the dynamics of these relationships requires further comprehensive study [11]. Regional features, quantitative characteristics and three-dimensional structure of climatic trends of interannual changes in the thermal characteristics of the study area are currently underestimated based on the totality of available observational data, modern assimilation models and reanalysis. In recent years, along with the deployment of remote autonomous observing systems and buoys, promising oceanographic data assimilation systems, such as SODA and GODAS [2], are being created, improved and increasingly used in ocean climate research. Thus, for 2000–2021 in the northwestern Pacific Ocean, the share of information entering the databases and the GODAS system from the observation network of ARGO diving buoys has sharply increased to 314,000 profiles (excluding

[2] Ministry of Natural Resources and Ecology of the Kamchatka Territory, 2021. [*Report on the State of the Environment in the Kamchatka Territory in 2020*]. Petropavlovsk-Kamchatsky, 385 p. Available at: https://kamgov.ru/files/6175d246c94f93.62211833.pdf [Accessed: 20 February 2023].

marginal seas) [20]. Further, in this work, the GODAS data precisely for this period were used.

The aim of the present research is to determine the trends and spatio-temporal features of interannual SST changes and water temperature of the upper 1,000-meter layer in the study area and to analyze their possible causal relationships with large-scale and regional processes in the ocean and atmosphere over certain phases of the modern 40-year global warming period. The use of a set of available observational data, modern assimilation models and reanalysis allowed to describe the three-dimensional structure of water temperature variability in different areas, to characterize the heterogeneity degree of the response of the water areas of the studied regions to ongoing global climate changes and to quantify their regional features.

Data and methods

To analyze interannual changes in water temperature, the data from optimal interpolation of sea surface temperature (SST on a 1°×1° grid) NOAA OI SST V2 for 1982–2021 was used (available at: https://psl.noaa.gov/data/gridded/data.noaa.oisst.v2.html), as well as potential temperature at different horizons from the GODAS oceanographic data assimilation system model [21] at 0.3° × 1° grid nodes (available at: https://www.esrl.noaa.gov/psd/data/gridded/data.godas.html) for 2000–2021 and materials from the constantly updated WOD18 database [20]. Data from reanalysis of pressure fields, wind and heat fluxes on the ocean surface and a series of climatic (circulation) indices [14]: AMO, NP, NPGO, PDO, SOI and WP, taking into account their seasonality, was also used. The data listed was obtained from the NOAA websites: https://psl.noaa.gov/data/gridded/index.html and https://psl.noaa.gov/data/climateindices/list/.

The statistics were calculated and the fields of anomalies of the studied series were decomposed into the main EOF components according to a unified method [4], supplemented by regression analysis. Also, according to the GODAS data, the anomalies of the integral temperature (ΔQ_T) (proportional to the heat content anomalies without taking into account the corresponding constants and volumetric characteristics) at the grid nodes for different layers from the surface to 950 m depth were calculated [18]. Taking into account the duration of summer and winter monsoons and the intraannual T_a and SST variation, conditionally warm summer (June – September), and conditionally cold winter (November – March) seasons (periods) of the year were chosen. Using data on the interannual variability (ΔQ_T) of the upper 5–200 m layer in the winter season, cluster analysis methods for the three main EOF components were used to identify four isolated areas located in different parts of the region water area: northeastern (NE), central (C), southeastern (SE) and southwestern (SW) (Fig. 1, *d*). Subsequently, by simple averaging of grid data in these areas, the long-term course of water temperature anomalies at each of the 31 GODAS horizons and the integral mean temperature in individual layers – upper, subsurface (5–200 m), intermediate (200–460 m) and deep (460–950 m) was calculated.

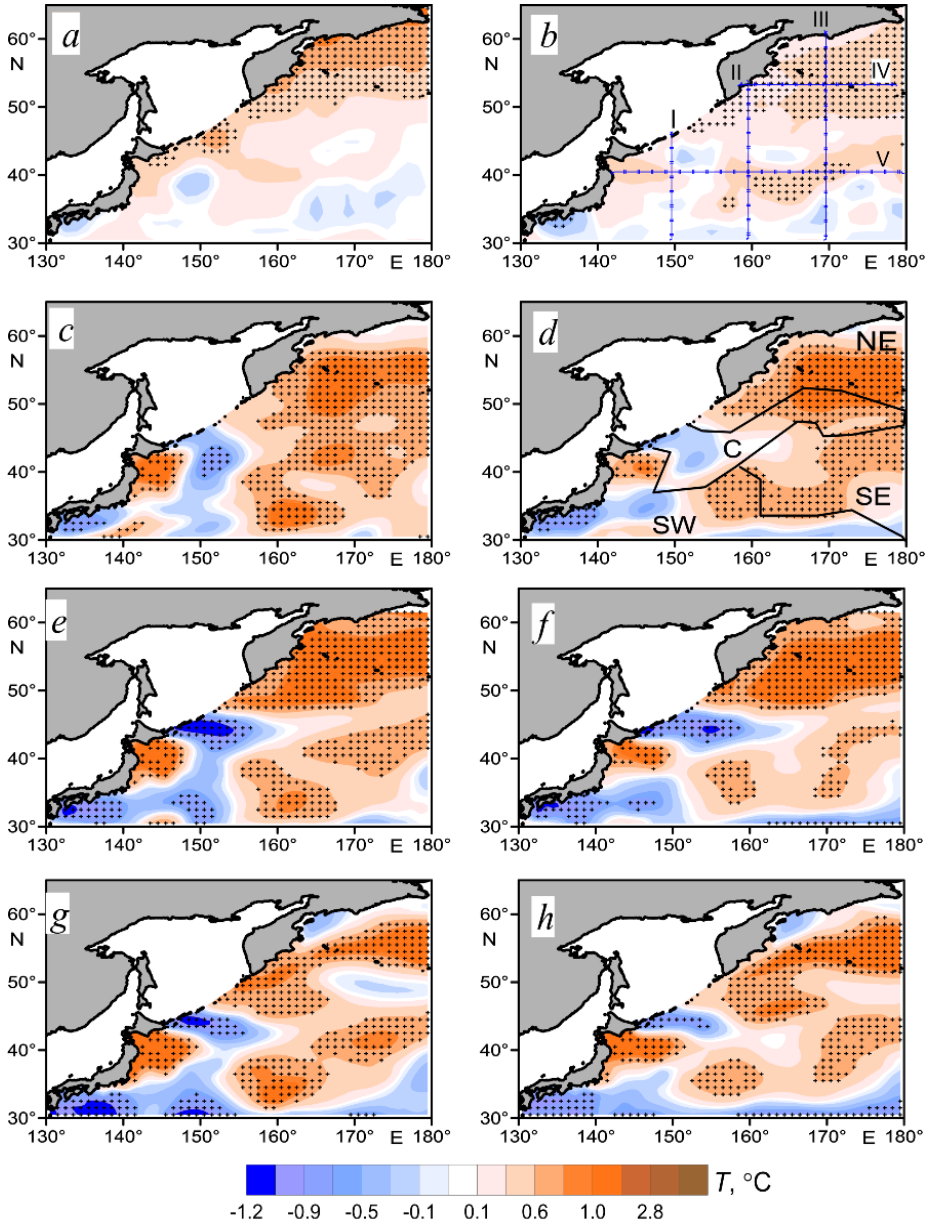

F i g. 1. Values of the SST, °C/10 years (*a*, *b*) and the normalized heat content anomalies (ΔQ_T) trends in the layers 5–200 m (*c*, *d*), 200–460 m (*e*, *f*) and 460–950 m (*g*, *h*) in the warm (left) and cold (right) seasons for 2000–2021. Here and below, crosses denote the grid nodes in which the estimates are statistically significant at the 95% level. Fragment *b* shows the location of sections (I–V), and fragment *d* – the identified areas (NE, C, SW, SE)

Features of spatial and interannual variability of water temperature

The location of the distinguished regions is generally consistent with the position of structural zones, frontal boundaries and the scheme of the main near-surface currents [9–11]. Thus, within the northeastern (NE) region boundaries, there

is a subarctic structure of waters, and within the southwestern (SW) region boundaries – a subtropical one. The central (C) region boundaries approximately correspond to the subarctic current and front location; the southeastern (SE) region corresponds to the transition zone or the mixing zone of subarctic and subtropical waters [9, 15]; the northern boundary of the southwestern (SW) region in the west is the mixing zone of the Oyashio and the northeastern branch of the Kuroshio [8], and to the east – to the Kuroshio Extension core, which passes into the North Pacific Current going to the east [16].

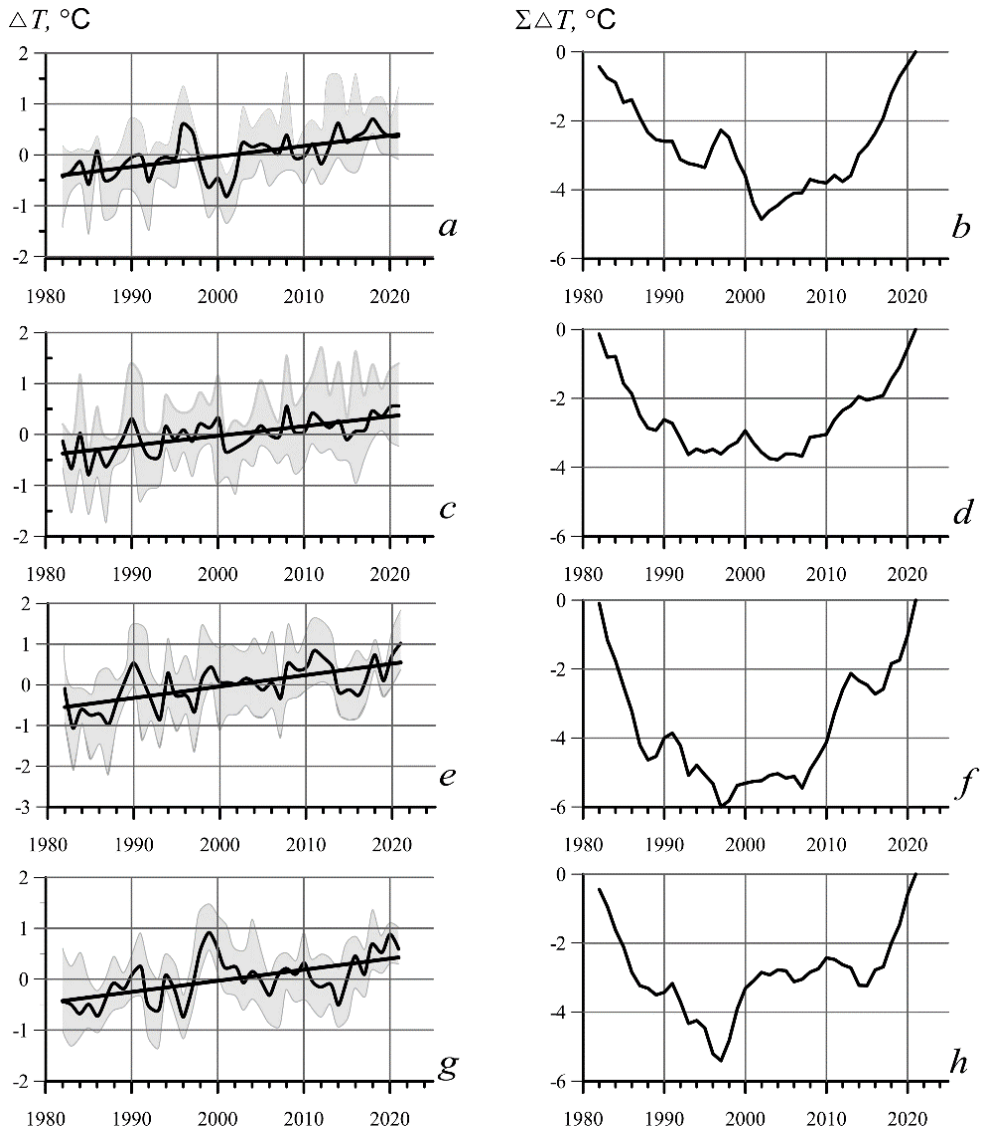

F i g. 2. Interannual variability of the annual average SST (ΔT) and the cumulative ($\sum\Delta T$) anomalies in the identified domains: NE (*a*, *b*), C (*c*, *d*), SE (*e*, *f*) and SW (*g*, *h*) in 1982–2021. The ranges of intra-year fluctuations, mean values over the region and linear trend (bold lines) are shown

The interannual changes in SST anomalies (SSTA) and accumulated SSTA in some areas over the entire 40-year period differ in the amplitude composition and synchronism of fluctuations (Fig. 2). In general, in both phases (periods) of climate change (1982–2000 and 2000–2021) in the region, positive statistically significant trends in the mean annual SST were observed. Their value in the first phase was 1.3–1.5 times higher than in the second one (Table 1). During the first phase, in the warm season, the areas of maximum positive statistically significant trends (~ 0.5–1.2 ºC/10 years) were located along the entire western boundary of the considered area and in the southwestern part of the water area; in the cold season, mainly in its southern sector, east of the coast of Japan (no Figure shown).

T a b l e 1

Trends of interannual changes of the SST anomalies in the identified domains for two periods: 1982–2000 and 2000–2021

Area	σ^2	*b*	*D*	*tr*	b_T/b_w	b_x/b_c
1982–2000						
NE	0.11	0.14	6	0.3	0.33	0.08
C	0.11	**0.35**	35	0.7	**0.48**	**0.45**
SE	0.24	0.42	23	0.8	0.45	**0.57**
SW	0.24	**0.54**	40	1.0	**0.56**	**0.59**
Whole area	0.09	**0.36**	45	0.7	**0.45**	**0.42**
2000–2021						
NE	0.13	**0.41**	52	0.9	**0.57**	**0.34**
C	0.07	**0.24**	34	0.5	0.27	0.18
SE	0.15	0.24	17	0.5	0.10	0.27
SW	0.12	0.17	9	0.4	0.12	0.15
Whole area	0.06	**0.26**	50	0.5	**0.26**	**0.23**

N o t e. σ^2 is variance of the average annual SST; *b* is the slope coefficient of the average annual temperature linear trend, °C for 10 years; *D* is the trend contribution to the total variance, %; *tr* is the trend over the observation period, °C; b_w, b_c are the values of *b* for the warm and cold seasons. Here and in the other tables, the statistically significant (95%) estimates are highlighted in bold.

During the second period, the value of positive trends on average over the entire water area decreased and the growth of SST slowed down (Table 1).

Unlike the SSTA trends, positive statistically significant trends in the warming of the 5–1000 m water column are observed over most of the study area (Fig. 1, *c* – *h*), which corresponds to modern regional and global trends [1] [2, 22]. The spatio-temporal features of the distribution of trends (ΔQ_T) in different layers are formed as a result of a complex interaction of various processes on the surface and in the depth of the ocean. The first three modes of expansion into the EOF field of interannual fluctuations of the integral temperature in the 5–200 m layer reflect the main features

of the internal structure of this field and describe most (~ 60%) of the total dispersion ΔQ_T.

The areas with negative and positive trends in ΔQ_T, located in the southwestern part of the study area, can be associated with the influence of local features of the hydrological regime and varied water exchange with the adjacent areas of the Philippine, Japan and Okhotsk seas. During this period, in the Kuroshio EAZO area, south of Japan, the largest fluxes and trends of sensible and latent heat on the sea surface and entire water column cooling of the 1000-m layer [12] were observed, as can be seen in Fig. 1, *c* – *h*. Another area with negative trends in ΔQ_T, located in the region of the central and southern Kuril Islands, could have formed as a result of an increase in the Oyashio Current and the inflow of colder waters from the Sea of Okhotsk [8, 11]. The area with positive trends in ΔQ_T, located south of Hokkaido Island and adjacent to the Sangar Strait was formed as a result of water exchange with the adjacent areas of the eastern Sea of Japan, where in recent decades an anomalous increase in heat content in the water column of the upper 300-m layer and an increase in discharges through the straits have been observed [23].

Interannual variability of thermal characteristics of the upper 1000-meter layer

Fig. 3 shows the vertical T_w distribution, its variability range and temperature trend at different horizons, averaged within the selected areas. The maximum values of seasonal T_w changes (2.6 °C) were observed in the cold season (Fig. 3, *h*) in the upper 50-meter layer of the SE region. As in other areas [12], the relationship between temperature changes at different horizons is manifested in the vertical profiles of T_w trends (Fig. 3, *c*, *f*, *i*, *l*). In the NE and SE regions, the entire water column warming of the upper 1000 m is observed in both seasons. Within the upper and intermediate layers, the trends have maximum values of 0.4–0.6ºC/10 years, which exceed the corresponding SST values (Table 1).

In other areas, the T_w trend signs alternate depending on the depth (Fig. 3, *f*, *l*). The maximum warming of the upper and intermediate layers occurred in the northeastern region and somewhat less in the southeastern region (increase by 18–20% and 5–8%, respectively), which is shown in Fig. 1 and Fig. 3. In general, over the past two decades, the heat content of the upper 1000-meter layer has increased by 3% in the study area.

Comparison of Fig. 1 and Fig. 4 allows to consider the features of the three-dimensional structure of temperature anomalies and warming/cooling trends both within each region and throughout the entire water area.

The northern zonal section IV along 53°N (Fig. 1, *b*) is entirely located in the northeastern region. In the water column of this section (no Figure shown), only positive T_w trend values were expressed in both seasons, which is fully consistent with the trend maps of the heat content of individual layers (Fig. 1) and the curves of the vertical distribution of the trend (Fig. 3). On the southern zonal section V at 40°N (Fig. 4, *a*) areas of warming of most of the water column in the SE and SW regions and a local cooling zone of the upper 300-m layer in the C region between them are observed.

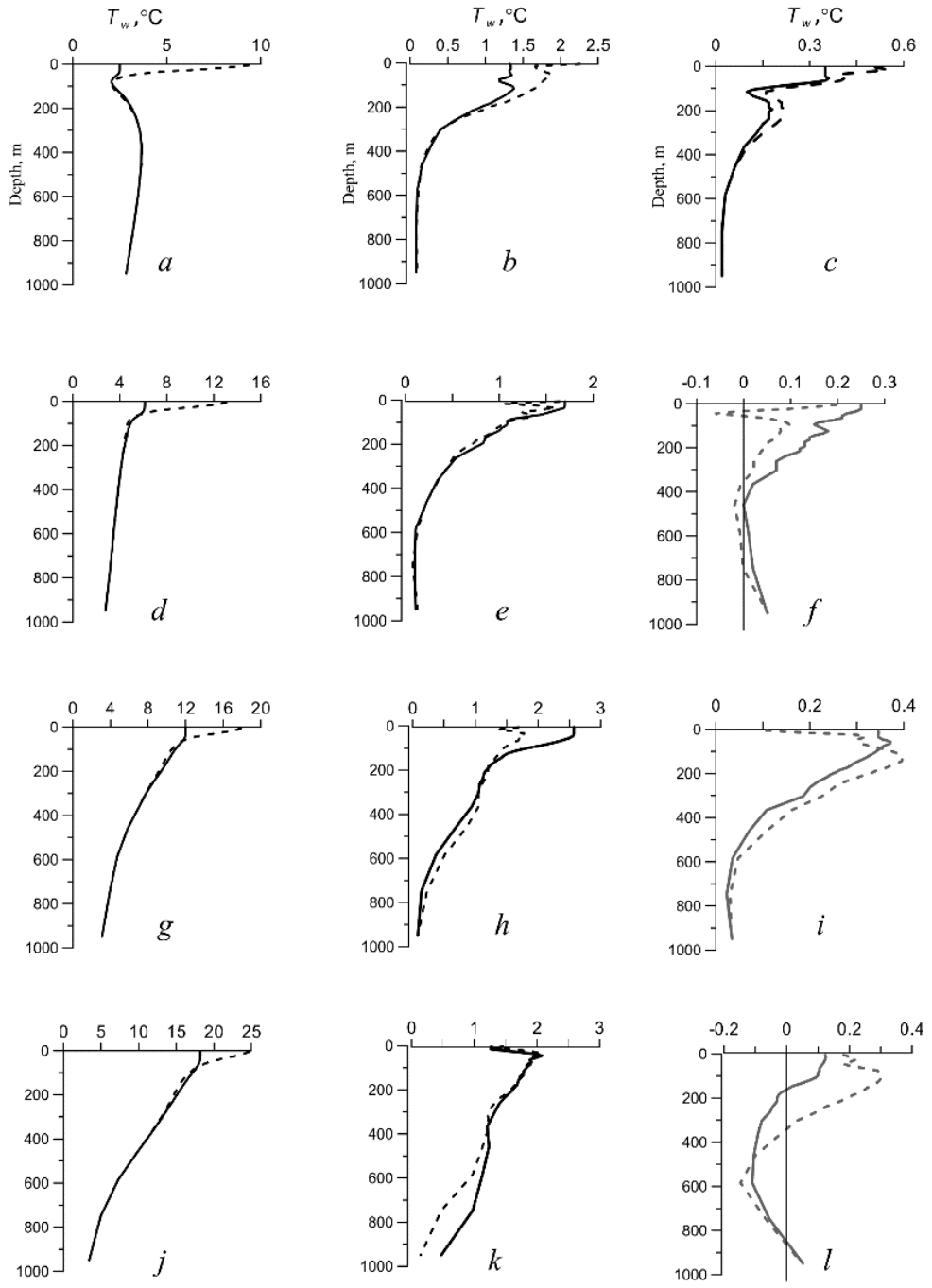

F i g. 3. Generalized curves of vertical distribution T_w (*a*, *d*, *g*, *j*), range of its changes (*b*, *e*, *h*, *k*) and trend (*c*, *f*, *i*, *l*) in the warm (dotted line) and cold (solid line) seasons in 2001–2021. From top to bottom: the areas NE, C, SE and SW

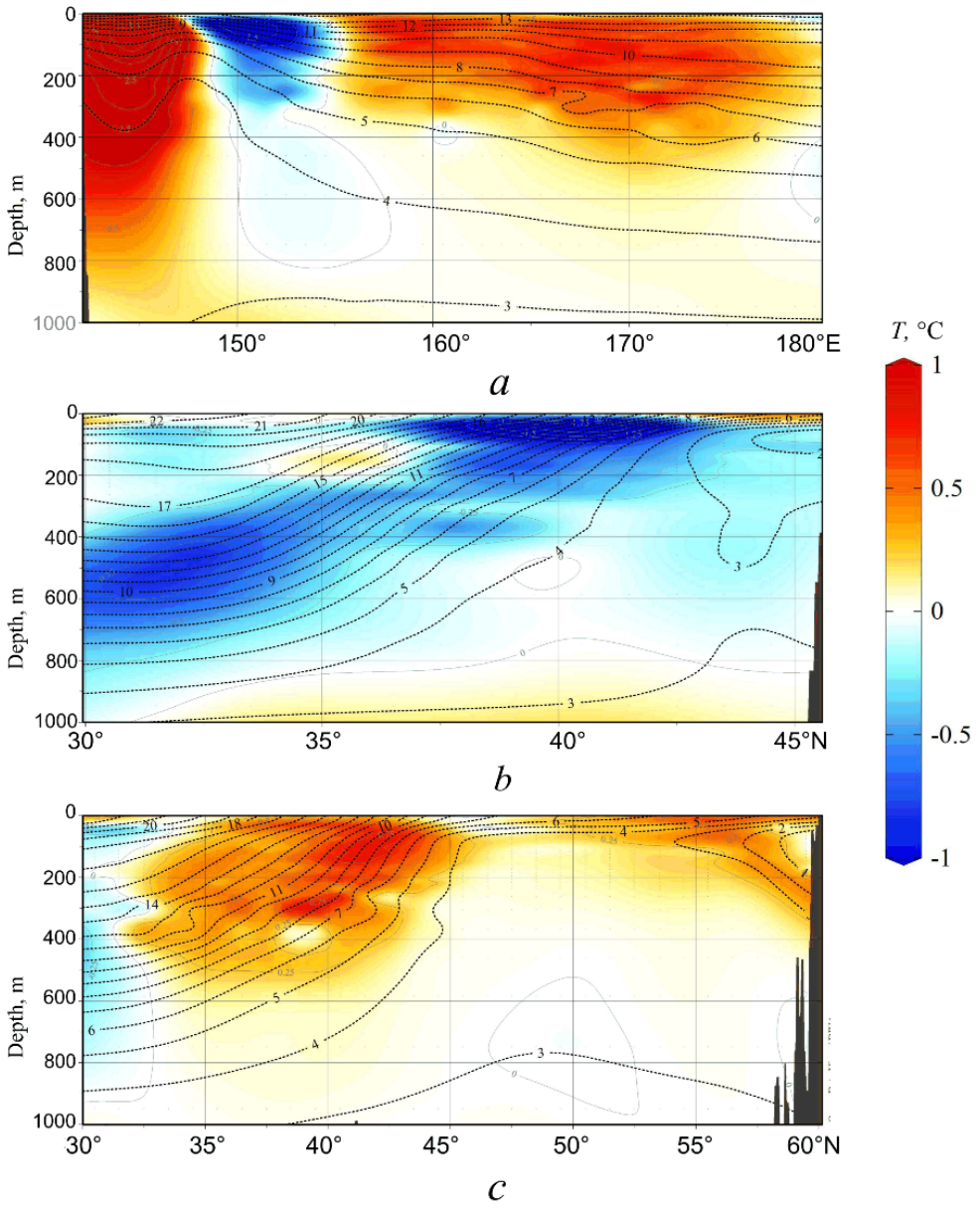

F i g. 4. Joint vertical distribution of the average annual T_w (dotted lines) and the temperature anomaly trends (highlighted in color) at the zonal V (at 40 °N) (*a*) and meridional I (at 150 °E) (*b*) and III (at 170 °E) (*c*) sections for the warm period in 2000–2021. The section locations are shown in Fig. 1, *b*

The meridional section I along 150°E (Fig. 4, *b*) crosses the C and SW regions. At the boundary of these regions, in the central part of the section, where the subarctic front zone is located, in the upper layer, the largest horizontal temperature gradients and the area of negative T_w trends, up to –0.8 ... –0.9 °C/10 years, are observed. Another area of greatest cooling is localized in the 300–600 m layer in the SW region, which significantly exceeds the penetration depth of seasonal

fluctuations from the surface [17]. The reason for this anomaly formation may be the advection of waters from the west. In this layer, negative T_w trends were noted in the water column of the Kuroshio EAZO south of Japan [12]. Positive statistically significant warming trends are not expressed in this section. The meridional section III along 170°E (Fig. 4, *c*) crosses the water area of all four identified areas. In the 800-m layer of its southern part, there is also an area with weakened negative T_w trends compared to those shown in section I. To the north of it, throughout the SE region, there is an area of maximum warming of the water column of the upper and intermediate layers, up to 0.5–0.7 ºC/10 years. The data from both sections are in good agreement with the trend maps of the heat content of individual layers (Fig. 1).

Correlations of thermal characteristics variability with large-scale and regional processes in the ocean and atmosphere

Correlations characterizing the influence of various circulation mechanisms and large-scale anomalies of baric and thermal fields in the ocean and atmosphere on the regional features of the thermal regime of the considered area are complex and diverse [4, 12, 24]. A cross-correlation and regression analysis of the time series of interannual SST anomalies and integral temperature anomalies (ΔQ_T) in the 0–200 m layer was carried out with climate indices and other parameters characterizing the state and dynamics of the climate system for two periods: 1982–2000 (the first period) and 2000–2021 (the second period).

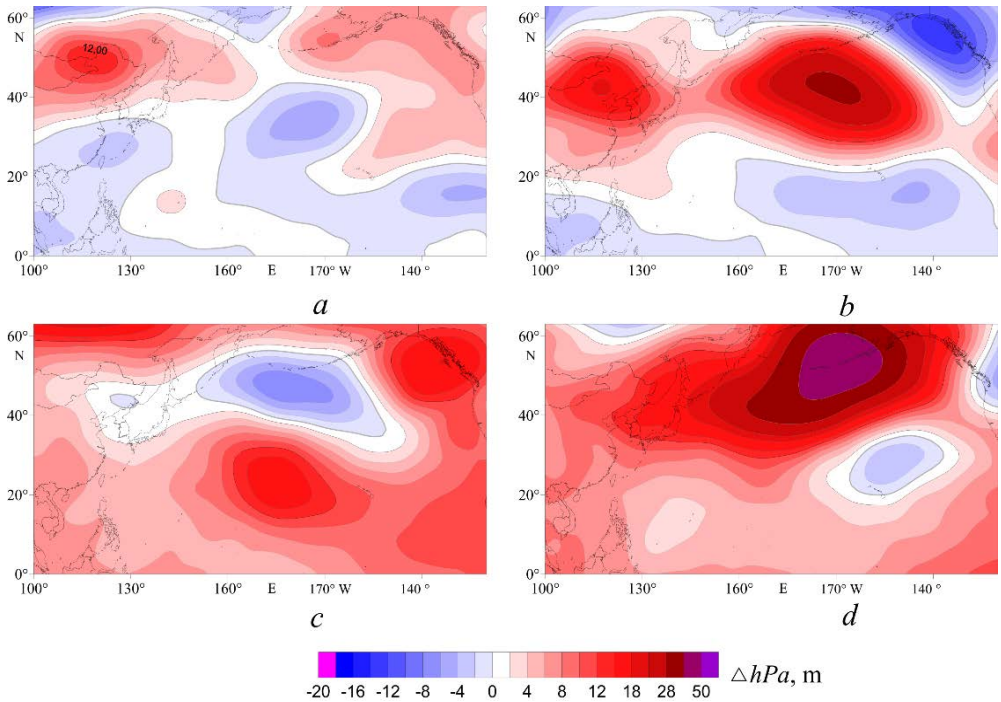

F i g. 5. Trends in the geopotential ΔH_{500} anomalies in 1980–2000 (*a*, *b*) and 2000–2021 (*c*, *d*) for the warm (left) and cold (right) seasons

One of the important climatic indicators characterizing the baric system state is the geopotential field of the isobaric surface of 500 hPa (AT_{500}) in the middle troposphere. Variations in the main EOF modes of geopotential anomalies (ΔH_{500}) in the region are closely related to SST fluctuations, the wind field and various climatic indices [4, 12]. In both seasons in 1982–2021 during the transition from the first to the second period, in most of the extratropical zone of the ocean, a trend sign change of ΔH_{500} anomalies and the formation of an area of its positive values in the region center, up to 3–4 dam/10 years, were observed (Fig. 5). During the transition from the first to the second period in the northern part of the study area during the cold season, a statistically significant weakening of the northern winds was observed and, as noted above, a decrease in SST trends in the entire water area by about 1.5 times.

Due to the atmospheric circulation restructuring, the value and sign of the trends in climate indices (*b*), as well as the nature of the correlations between SST fluctuations and the most significant CI, also changed (Table 2).

T a b l e 2

Correlation coefficients of SST in the identified areas with climate indices (CI) for the warm and cold (in brackets) seasons for two periods during 1982–2021

Index and areas	$K_1\Delta H_{500}$	PDO	NP	AD	AMO	NPGO	IPO
1982–2000							
b	0.1 (0.4)	0.5 (-0.7)	-(0.6)	-0.2 (-)	**0.2** (**0.1**)	0.1 (0.0)	-0.4 (-0.4)
NE	-0.4 (0.1)	0.2 (0.2)	- (0.1)	0.1 (-)	0.1 (0.1)	-0.3 (-0.4)	0.1 (0.2)
C	0.2 (0.3)	**-0.7** (**-0.7**)	- (0.3)	**-0.5** (-)	0.2 (**0.5**)	0.4 (0.0)	**-0.6** (-0.1)
SE	**0.6** (**0.5**)	**-0.9** (**-0.9**)	- (**0.5**)	**-0.5** (-)	0.3 (0.3)	0.4 (0.0)	**-0.7** (-0.3)
SW	**0.6** (0.1)	**-0.8 (-0.6**)	- (0.3)	**-0.6** (-)	**0.5** (**0.6**)	**0.7** (-0.3)	**-0.6** (-0.2)
Whole area	0.4 (0.4)	**-0.8** (**-0.8**)	- (0.4)	**-0.5** (-)	0.4 (**0.5**)	0.4 (0.0)	**-0.6** (-0.2)
2000–2021							
b	**0.7** (**0.6**)	0.3 (0.4)	- (**1.4**)	0.0 (-)	0.0 (0.0)	**-1.5** (-1.**6**)	0.0 (0.2)
NE	0.3 (**0.6**)	0.2 (0.3)	- (**0.4**)	0.0 (-)	0.3 (0.2)	-0.4 (**-0.8**)	-0.1 (0.2)
C	0.2 (**0.6**)	-0.3 (**-0.5**)	- (**0.6**)	0.0 (-)	0.2 (-0.1)	0.0 (**-0.4**)	-0.4 (-0.3)
SE	-0.1 (**0.6**)	**-0.7** (**-0.6**)	- (**0.6**)	0.3 (-)	0.1 (0.0)	0.4 (-0.2)	-0.4 (**-0.5**)
SW	**-0.5** (-0.2)	-0.1 (-0.3)	- (0.1)	0.2 (-)	-0.2 (0.2)	-0.2 (-0.1)	-0.4 (-0.1)
Whole area	0.3 (**0.6**)	-0.3 (**-0.4**)	- (**0.7**)	-0.3 (-)	0.2 (0.1)	-0.1 (**-0.5**)	**-0.5** (-0.3)

N o t e. *b* is the slope coefficient of the CI linear trend, conv. units/10 years; ($K_1\Delta H_{500}$) are the EOF time coefficients of the first mode of geopotential anomaly variations.

Table 2 data indicates a significantly heterogeneous nature of the relationships between the interannual SST variability and large-scale processes (CI), which in different regions are consistent only in the sign of the correlation coefficients. In general, in the region during the second period (2000–2021), the influence on SST of such indicators of atmospheric and ocean dynamics as $K_1\Delta H_{500}$, NP, WP and NPGO increased. However, the impact of PDO, AD, AMO and IPO weakened during this period. The mechanisms of these processes involved in the formation of anomalies in the SST fields, heat content and their anomalies are the subject of independent and numerous studies, during which it was shown that the thermal structure of the upper layer is determined mainly by the heat budget on the surface, fluctuations of wind, currents, and remote influence. In the intermediate and deep layers, the influence of advection and water mixing is reflected to a greater extent [2, 12, 13, 22, 25]. Compared with SST, the most significant (in terms of area of influence, duration and the correlation coefficient value) in the last two decades, the corresponding correlations of variations in the integral temperature in the 5–200 m layer and various indices are manifested with the following CI: NPGO, PDO, WP, PTW and also with $K_1\Delta H_{500}$ (Fig. 6).

It is interesting to note that statistically significant correlations of SOI with fluctuations in heat content and SST are not expressed in the considered area.

In the southwestern part of the water area, there are also statistically significant relationships between variations in ΔQ_T (5–200 m) and the values of sensible (SH) and latent (LH) heat fluxes on the surface in the Kuroshio EAZO area in the northern Philippine Sea [12], as well as relationships of thermal conditions with the Kuroshio axis position, its intensity and thermal characteristics [2, 15, 22, 25–27]. Here, in the latitude band between 25° and 45°N, the ocean transfers to the atmosphere through these streams ~ 70% of the heat accumulated in the equatorial zone [24].

In general, the first three EOF modes of interannual fluctuations in the field of anomalies of the integral temperature of the upper 5–200 m layer (ΔQ_T) describe the main features of its structure, 60% variability (less than for SST) and are closely related to large-scale processes in the ocean and atmosphere (Table 3).

Correlations of interannual fluctuations in ΔQ_T in the upper layer with different CI weaken as the mode number and its contribution to the total variance of the integral temperature variability increase. In the underlying layers, these relationships appear with a time lag of 6–12 months or more, which is associated with large-scale features of the ocean and atmosphere circulation in the study area [2, 28]. Estimates of the values of the multiple regression (the proportion of the explained variance D, %) coefficients of the contribution of the set of various climatic variables' (CI) fluctuations for the warm and cold (in parentheses) seasons and the first – third EOF modes of the average annual anomalies of the integral heat content in the 5–200 m layer are given below:

$-K_1\Delta Q_T$: NPGO, ($K_1\Delta H_{500}$), PNA, WP, $K_2\Delta H_{500}$, (NP): D = 79%,

$-K_2\Delta Q_T$: PDO, ($K_2\Delta H_{500}$), (EP-NP), LH, $K_3\Delta H_{500}$, PTW: D = 70%,

–$K_3\Delta Q_T$: (WP), (SH), (LH): D = 63%.

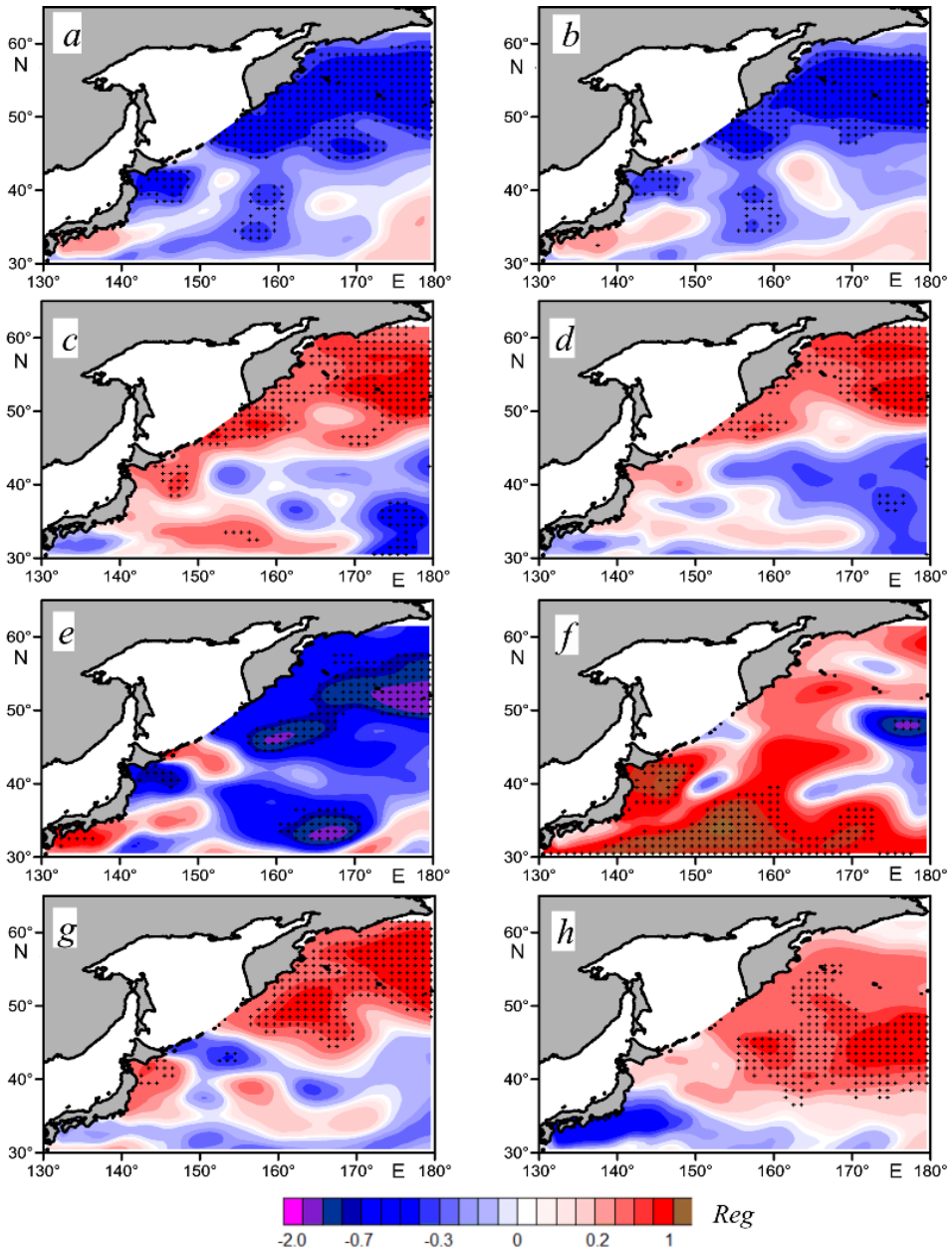

F i g. 6. Linear regression coefficients (*Reg*) of fluctuations in anomalies of the annual average values of the integral temperature (ΔQ_T) in the 5–200 m layer with the climatic indices: NPGO (*a*, *b*), PDO (*c*, *d*), WP (*e*, *f*) and $K_1\Delta H_{500}$ (*g*, *h*) in the warm (*left*) and cold (*right*) seasons, 2000–2021

Table 3

Correlation coefficients of the EOF modes of average annual integral temperature anomalies in the 5–200 m layer with different CI in 2000–2021

Index	PDO	WP	NP (x)	NPGO	PNA	$K_1\Delta H_{500}$	$K_2\Delta H_{500}$
$K_1\Delta Q_T$	0.3 (0.3)	**-0.5** (0.2)	- (**0.4**)	**-0.7** (**-0.7**)	**0.5** (-0.4)	**0.5** (**0.6**)	**-0.5** (0.4)
$K_2\Delta Q_T$	**-0.6** (**-0.6**)	0.0 (0.2)	- (0.3)	0.4 (0.3)	0.1 (-0.2)	-0.1 (0.1)	0.3 (**0.5**)
$K_3\Delta Q_T$	0.1 (0.0)	0.0 (**0.8**)	- (-0.1)	-0.1 (-0.1)	0.3 (0.4)	0.2 (-0.4)	-0.3 (0.1)

N o t e. K_1, K_2, and K_3 are the time coefficients of the EOF first modes of decomposition of the ΔQ_T and ΔH_{500} fields.

Here, the CI are arranged in descending order of the statistical significance of the regression relationships with each of the modes. The greatest contribution to the first mode variability is provided by the processes parameterized by NPGO [13], the second by PDO and the third by WP [14]. The mechanisms of these connections are complex and ambiguous. Several studies have noted that since the 1990s in the northern Pacific Ocean, the subarctic (subpolar) circulation intensification took place, as well as expansion and poleward shift of the subtropical circulation and the trajectories of cyclones and typhoons [1] [10, 16, 25], which are becoming more frequent [29]. One of the indicators of the ten-year dynamics of the system of currents in the region is the NPGO index. In its trends, significant negative trends in the last two decades were monitored (Table 2). The NPGO fluctuations reflect the change in the intensity of the large-scale North Pacific cyclonic gyre [13]. Its fluctuations are due to variations in wind upwelling and horizontal advection on regional and basin scales and are part of the climate variability regime, which is manifested in the trends in ocean level fluctuations [25], SST and heat content (Tables 2, 3, Fig. 6, *a*, *b*). The NPGO variability has a remote and delayed effect on the Kuroshio-Oyashio Current system and adjacent areas of the Western Pacific Ocean with some phase delay.

During the study period, the frequency of El Niño and La Niña events also remains subject to internal ten-year variability, but without a pronounced long-term trend in their intensity and statistically significant relationships with fluctuations in thermal characteristics in the study area are not expressed.

The deepening of the positive anomalies' area in the pressure field trend (AT_{500} geopotential) in the northeastern part of the ocean in recent decades indicates a weakening of the Aleutian depression, a restructuring of the atmospheric (*NP* index) and oceanic (NPGO index, which is an oceanic expression of NP [2, 13]) circulation and is accompanied by water column warming in most of the study area (Table 2, Fig. 1).

The Pacific Decadal Oscillation (PDO) is also the dominant factor in the SST variability in the North Pacific on a decadal time scale [30, 31]. Due to increased stratification in the global warming process at the beginning of the 20th century the decadal PDO variability is significantly suppressed, its amplitude decreases, and

the decadal cycle shifts to a higher frequency band [32]. During this period, the PDO effect on SST decreased and manifested only in relation to the second mode of heat content (Tables 2, 3). Similar tendencies of weakening to statistically insignificant correlations of SST and EOF modes of the heat content of the upper layer are observed both for the AMO and IPO indices – the Atlantic and Pacific interdecadal fluctuations, and for AD – the Asian depression.

Conclusion

At the turn of the 20th–21st centuries, separate periods with different rates of warming are observed. They are formed during changes in climatic regimes, in large-scale atmospheric and oceanic circulation and depend on remote influences and local physical and geographical conditions. These processes led to a significant restructuring of the SST fields and the heat content of various layers in the sea water column, the formation of large-scale anomalies, and are differently expressed in both phases of interannual variability and in individual parts of the water area of the considered region.

In both phases of climate change (1982–2000 and 2000–2021) in the region, positive statistically significant trends in the average annual SST were generally observed, the value of which in the first phase was 1.3–1.5 times higher than in the second. During the first phase, the maximum rate of sea surface warming was observed in the warm season in certain areas of the western Bering Sea, near the eastern coast of Kamchatka and the Kuril Islands and in the southwestern part of the water area, in the cold season – mainly in its southern sector, to the east of the Honshu Island coast. During the warm season of the second phase, the area of the region with positive SST trends significantly decreased and localized in the northwestern part of the considered water area.

Unlike the SST trends, positive statistically significant trends in water temperature in different layers of the underlying 5–1,000 m water column can be observed in most of the study area, which indicates a coincidence with modern trends in other regions. East of 155°N in this depth range, warming of the entire layer is observed. Here, temperature trends are positive in both seasons, and in the upper and intermediate layers their values reach maximum values of 0.4–0.6 ºC/10 years, which was reflected in an increase in the heat content of these layers in the northeastern part of the study area by 18–20%, in the southeastern part – by 5–8%. In other areas, small negative T_w trends are observed in the near-surface layer and cooling of the intermediate and deep layers.

Variations in the main EOF modes of the geopotential anomalies (ΔH_{500}) in the North Pacific Ocean are closely related to the SST fluctuations, wind field and various climatic indices. In general, in the region during the second period (2000–2021), the influence on SST of such indicators of the characteristics of the baric field and the ocean state as geopotential anomalies ΔH_{500}, NP, WP and NPGO increased. During this period, the corresponding correlations of variations in the heat content of the upper layer appear with the following CI: NPGO, PDO, WP, PTW, as well as with the most energy-carrying EOF modes ΔH_{500}. In the intermediate layer, they decay and remain only for WP and EOF ΔH_{500}. In the considered area, statistically significant SOI relationships with both fluctuations in heat content and SST are not expressed.

REFERENCES

1. Johnson, G.C. and Lyman, J.M., 2020. Warming Trends Increasingly Dominate Global Ocean. *Nature Climate Change*, 10, pp. 757-761. doi:10.1038/s41558-020-0822-0
2. Na, H., Kim, K.-Y., Minobe, S. and Sasaki, Y.N., 2018. Interannual to Decadal Variability of the Upper-Ocean Heat Content in the Western North Pacific and Its Relationship to Oceanic and Atmospheric Variability. *Journal of Climate*, 31(13), pp. 5107-5125. doi:10.1175/JCLI-D-17-0506.1
3. Stephens, C., Levitus S., Antonov, J. and Boyer, T.P., 2001. On the Pacific Ocean Regime Shift. *Geophysical Research Letters*, 28(19), pp. 3721-3724. doi:10.1029/2000GL012813
4. Rostov, I.D., Dmitrieva, E.V. and Rudykh, N.I., 2021. Climatic Changes of Thermal Conditions in the Pacific Subarctic at the Modern Stage of Global Warming. *Physical Oceanography*, 28(2), pp. 149-164. doi:10.22449/1573-160X-2021-2-149-164
5. Meehl, G.A., Hu, A., Arblaster, J.M., Fasullo, J. and Trenberth, K.E., 2013. Externally Forced and Internally Generated Decadal Climate Variability Associated with the Interdecadal Pacific Oscillation. *Journal of Climate*, 26(18), pp. 7298-7310. doi:10.1175/jcli-d-12-00548.1
6. Loeb, N.G., Thorsen, T.J., Norris, J.R., Wang, H. and Su, W., 2018. Changes in Earth's Energy Budget during and after the "Pause" in Global Warming: An Observational Perspective. *Climate*, 6(3), 62. doi:10.3390/cli6030062
7. Nieves, V., Willis, J.K. and Patzert, W.C., 2015. Recent Hiatus Caused by Decadal Shift in Indo-Pacific Heating. *Science*, 349(6247), pp. 532-535. doi:10.1126/science.aaa4521
8. Foux, V.R. and Michurin, A.N., eds., 1997. [*Origins of Oiyasio*]. Saint Petersburg: St. Petersburg University Publishing, 248 p. (in Russian).
9. Favorite, F., Dodimead, A.J. and Nasu, K., 1976. *Oceanography of the Subarctic Pacific Region, 1960-71*. Vancouver, Canada: International North Pacific Fisheries Commission, Bulletin No. 33. Japan, Tokyo: Kenkyusha Printing Company, 187 p. [online] Available at: http://www.npafc.org/new/inpfc/INPFC%20Bulletin/Bull%20No.33/Bulletin%2033.pdf
10. Kuroda, H., Suyama, S., Miyamoto, H., Setou, T. and Nakanowatari, T., 2021. Interdecadal Variability of the Western Subarctic Gyre in the North Pacific Ocean. *Deep Sea Research Part I: Oceanographic Research Papers*, 169, 103461. doi:10.1016/j.dsr.2020.103461
11. Yasuda, I., 2003. Hydrographic Structure and Variability in the Kuroshio-Oyashio Transition Area. *Journal of Oceanography*, 59, pp**.** 389-402. doi:10.1023/A:1025580313836
12. Rostov, I.D., Dmitrieva, E.V. and Rudykh, N.I., 2022. Interannual Variability of Thermal Conditions in the Kuroshio Energetically Active Zone and Adjacent Areas of the Philippine Sea. *Russian Meteorology and Hydrology*, 47, pp. 290-303. doi:10.3103/S1068373922040057
13. Di Lorenzo, E., Schneider, N., Cobb, K.M., Franks, P.J.S., Chhak, K., Miller, A.J., McWilliams, J.C., Bograd, S.J., Arango, H., Curchitser, E., Powell, T.M. and Rivière, P., 2008. North Pacific Gyre Oscillation Links Ocean Climate and Ecosystem Change. *Geophysical Research Letters*, 35(8), L08607. doi:10.1029/2007GL032838
14. Panin, G.N., Vyruchalkina, T.Yu. and Solomonova, I.V., 2010. Regional Climatic Changes in Northern Hemisphere and Their Relationship to Circulation Indexes. *Problems of Ecological Monitoring and Ecosystem Modelling*, 23, pp. 92-108 (in Russian).
15. Belkin, I., Krishfield, R. and Honjo, S., 2002. Decadal Variability of the North Pacific Polar Front: Subsurface Warming versus Surface Cooling. *Geophysical Research Letters*, 29(9), pp. 65-1-65-4. doi:10.1029/2001GL013806
16. Qiu, B., 2002. Large-Scale Variability in the Midlatitude Subtropical and Subpolar North Pacific Ocean: Observations and Causes. *Journal of Physical Oceanography*, 32(1), pp. 353-375. doi:10.1175/1520-0485(2002)032<0353:LSVITM>2.0.CO;2
17. Byshev, V.I., Figurkin, A.L. and Anisimov, I.M., 2016. Recent Climate Changes of Thermohaline Structure in the North-West Pacific. *Izvestiya TINRO*, 185(2), pp. 215-227 (in Russian).

18. Rostov, I.D. and Dmitrieva, E.V., 2021. Regional Features of Interannual Variations in Water Temperature in the Subarctic Pacific. *Russian Meteorology and Hydrology*, 46, pp. 106-114. doi:10.3103/S1068373921020059

19. Piuchugin, M.K., Gurvich, I.A., Khazanova, E.S. and Salyuk, P.A., 2020. Some Features of Oceanological Conditions of the Microalgae Autumn-Flowering near the Southeast Shore of Kamchatka. *Underwater Investigation and Robotics*, 4(34), pp. 70-73. doi:10.37102/24094609.2020.34.4.010

20. Boyer, T.P., Baranova, O.K., Coleman, C., Garcia, H.E., Grodsky, A., Locarnini, R.A., Mishonov, A.V., Paver, C.R., Reagan, J.R. [et al.], 2018. World Ocean Database 2018. In: A. V. Mishonov, technical ed., 2018. *NOAA Atlas NESDIS 87*. [online] Available at: https://www.ncei.noaa.gov/products/worldocean-database [Accessed: 9 June 2022].

21. Penny, S.G., Behringer, D.W., Carton, J.A. and Kalnay, E., 2015. A Hybrid Global Ocean Data Assimilation System at NCEP. *Monthly Weather Review*, 143(11), pp. 4660-4677. doi:10.1175/MWR-D-14-00376.1

22. Hu, Z., Hu, A., Hu, Y. and Rosenbloom, N., 2020. Budgets for Decadal Variability in Pacific Ocean Heat Content. *Journal of Climate*, 33(17), pp. 7663-7678. doi:10.1175/JCLI-D-19-0360.1

23. Na, H., Kim, K.-Y., Chang, K.-I., Park, J.J., Kim, K. and Minobe, S., 2012. Decadal Variability of the Upper Ocean Heat Content in the East/Japan Sea and Its Possible Relationship to Northwestern Pacific Variability. *Journal of Geophysical Research*, 117(C2), C02017. doi:10.1029/2011JC007369

24. Kwon, Y.-O., Alenxader, M.A., Bond, N.A., Frankignoul, C., Nakamura, H., Qiu, B. and Thompson, L.A., 2010. Role of the Gulf Stream and Kuroshio–Oyashio Systems in Large-Scale Atmosphere–Ocean Interaction: A Review. *Journal of Climate*, 23(12), pp. 3249-3281. doi:10.1175/2010JCLI3343.1

25. Ceballos, L.I., Di Lorenzo, E., Hoyos, C.D., Schneider, N. and Taguchi, B., 2009. North Pacific Gyre Oscillation Synchronizes Climate Fluctuations in the Eastern and Western Boundary Systems. *Journal of Climate*, 22(19), pp. 5163-5174. doi:10.1175/2009JCLI2848.1

26. Hasegawa, T., Yasuda, T. and Hanawa, K., 2007. Multidecadal Variability of the Upper Ocean Heat Content Anomaly Field in the North Pacific and Its Relationship to the Aleutian Low and the Kuroshio Transport. *Papers in Meteorology and Geophysics*, 58, pp. 155-166. doi:10.2467/mripapers.58.155

27. Wang, Y-L. and Wu, Ch.-R., 2019. Enhanced Warming and Intensification of the Kuroshio Extension, 1999–2013. *Remote Sensing*, 11(1), 101. doi:10.3390/rs11010101

28. Nonaka, M., Nakamura, H., Tanimoto, Y., Kagimoto, T. and Sasaki, H. 2008. Interannual-to-Decadal Variability in the Oyashio and Its Influence on Temperature in the Subarctic Frontal Zone: An Eddy-Resolving OGCM Simulation. *Journal of Climate*, 21(23), pp. 6283-6303. doi:10.1175/2008JCLI2294.1

29. Chand, S.S., Tory, K.J., Ye, H. and Walsh, K.J.E, 2017. Projected Increase in El Niño-Driven Tropical Cyclone Frequency in the Pacific. *Nature Climate Change*, 7, pp. 123-127. doi:10.1038/nclimate3181

30. Kumar, A. and Wen, C., 2016. An Oceanic Heat Content-Based Definition for the Pacific Decadal Oscillation. *Monthly Weather Review*, 144(10) pp. 3977-3984. doi:10.1175/mwr-d-16-0080.1

31. Newman, M., Alexander, M.A., Ault, T.R., Cobb, K.M., Deser, C., Di Lorenzo, E., Mantua, N.J., Miller, A.J., Minobe, S. [et al.], 2016. The Pacific Decadal Oscillation, Revisited. *Journal of Climate*, 29(12), pp. 4399-4427. doi:10.1175/jcli-d-15-0508.1

32. Geng, T., Yang, Y. and Wu, L., 2019. On the Mechanisms of Pacific Decadal Oscillation Modulation in a Warming Climate. *Journal of Climate*, 32(5), pp. 1443-1459. doi:10.1175/jcli-d-18-0337.1

About the authors:

Igor D. Rostov, Head of the Informatics and Ocean Monitoring Laboratory, FSBSI V.I. Il'ichev Pacific Oceanological Institute, Far Eastern Branch, Russian Academy of Sciences (43 Baltiyskaya Str., Vladivostok, 690041, Russian Federation), Ph.D. (Geogr.), **ORCID ID: 0000-0001-5081-7279**, rostov@poi.dvo.ru

Elena V. Dmitrieva, Senior Research Associate, Informatics and Ocean Monitoring Laboratory, FSBSI V.I. Il'ichev Pacific Oceanological Institute, Far Eastern Branch, Russian Academy of Sciences (43 Baltiyskaya Str., Vladivostok, 690041, Russian Federation), Ph.D. (Techn. Sci.), **ORCID ID: 0000-0002-0094-5296**, e_dmitrieva@poi.dvo.ru

Natalya I. Rudykh, Senior Research Associate, Informatics and Ocean Monitoring Laboratory, FSBSI V.I. Il'ichev Pacific Oceanological Institute, Far Eastern Branch, Russian Academy of Sciences (43 Baltiyskaya Str., Vladivostok, 690041, Russian Federation), Ph.D. (Geogr.), **ResearcherID: N-5821-2018**, rudykh@poi.dvo.ru

Contribution of the co-authors:

Igor D. Rostov – development of the article structure, processing and analysis of the data, writing the article text.

Elena V. Dmitrieva – collection and processing of oceanographic data, calculations, drawing design, text editing.

Natalya I. Rudykh – collection and processing of initial data on meteorological stations, calculations, editing of text and references.

The authors have read and approved the final manuscript.
The authors declare that they have no conflict of interest.